Catalysis Today xxx (xxxx) xxx

Contents lists available at ScienceDirect

Catalysis Today

journal homepage: www.elsevier.com/locate/cattod

Hydrogenation of dimethyl oxalate to ethylene glycol on Cu/SiO_2 catalysts prepared by a deposition-decomposition method: Optimization of the operating conditions and pre-reduction procedure

Gianfranco Giorgianni [a,*], Chalachew Mebrahtu [b], Siglinda Perathoner [c], Gabriele Centi [c], Salvatore Abate [c,*]

[a] Laboratory of Industrial Chemistry and Catalysis, University of Calabria, Via P. Bucci, I-87036 Rende, Cosenza, Italy
[b] Institute for Technical and Macromolecular Chemistry (ITMC), RWTH Aachen University, Worrigerweg 2, 52074 Aachen, Germany
[c] Department of ChiBioFarAm (Industrial Chemistry), University of Messina, ERIC aisbl and INSTM/CASPE, V.le F. Stagno D'Alcontres 31, 98166 Messina, Italy

ARTICLE INFO

Keywords:
Hydrogenation
Dimethyl oxalate
Ethylene glycol
FTIR
Optimization
Cu/SiO_2

ABSTRACT

Cu/SiO_2 catalysts prepared by a deposition-decomposition (DD) method using ammonium hydroxide are currently among the most promising catalysts for oxalates hydrogenation to ethylene glycol (EG). Here, a Cu/SiO_2 catalyst prepared by the DD method was pre-reduced at a) 200–350 °C in 100% H_2, and 2) 200 °C in a 50% H_2/N_2 mixture. Then, it was tested at 200 °C, and 25 barg, while EG yields were optimized, with H_2-GHSV and H_2/DMO ratios in the ranges 1000–4000 h^{-1} and 30–200 mol/mol. The calcined catalyst presents an XRD amorphous Cu phyllosilicate phase. After pre-reduction in pure H_2 at 200–250 °C (T_{red}), the Cu metallic surface area increased from 6 to 12 m^2/g_{cat} and slightly decreased at 350 °C. Simultaneously, the silanol's band, measured by DRIFT experiments, increased with T_{red}. The highest ethylene glycol yield (91%) was achieved after pre-reduction at 200 °C in pure hydrogen, working with an H_2-GHSV and H_2/DMO of 1050 h^{-1} and 68 mol/mol, respectively. The catalyst was stable for more than 36 h after a 20 h induction period. Catalyst characterization results as a function of T_{red} confirm that mixed-valence copper nanoparticles favor the EG selective formation, while side reactions leading to ethanol and 1,2-butanediol are related to exposed acidic and basic sites due to decreased Cu/support interactions.

1. Introduction

Ethylene glycol (EG) is a bulk chemical used mainly as an anti-freezing agent, solvent, and monomer to produce polyesters. Its world-wide production capacity, mostly located in China, in 2019 was 41.8 Mt/y, with a forecast increase of 55% by 2024 [1]. However, it is still mostly produced by the hydration of oil-based ethylene oxide. The increasing demand to produce EG, the fluctuating oil market, and the need to decrease its environmental impact are pushing the research toward the *two-steps indirect synthesis of EG*, employing syngas from coal, natural gas [2–4] or biomass for the production of Dimethyl (DMO) and diethyl (DEO) oxalates and their catalytic hydrogenation to EG. Even though DEO production from syngas was industrialized in China in 2010 [5], the intrinsically safer production of DMO makes its production and hydrogenation preferable [4]. Although the Coal-to-EG route was already industrialized in China, the poor stability and selectivity of the catalysts employed for the hydrogenation of DMO still limit the potential benefits from this route [6]. The DMO hydrogenation is a two-step hydrogenation reaction where it is first hydrogenated to methyl glycolate (MG) and the latter to EG (Scheme 1).

The DMO hydrogenation was initially studied in the liquid phase, using homogenous $Ru(CO)_2(Ac_2)(PBu)_3$ catalysts [7–11]. However, the issue of catalyst separation and the high H_2 pressure needed oriented the research toward the vapor phase hydrogenation of oxalates. The latter was mainly studied with Cu-based catalysts due to its high selectivity in the hydrogenation of esters to alcohols and inactivity for the hydrogenolysis of carbon-carbon bonds [12]. Although the use of improved Raney Cu catalysts [13] was also reported, due to the sintering-prone behavior of Cu and its low activity, Cu is rarely used by itself [14]. The best catalyst's stability for the hydrogenation of DMO, was obtained with Cu-Cr catalysts [15]. However, due to chromium toxicity, more environmentally friendly catalysts are being developed. Among these,

* Corresponding authors.
E-mail addresses: gianfranco.giorgianni@unical.it (G. Giorgianni), abates@unime.it (S. Abate).

https://doi.org/10.1016/j.cattod.2021.08.032
Received 4 August 2021; Accepted 26 August 2021
Available online 31 August 2021

interesting results were reported for Cu/SiO_2 [16], bimetallic core-shell Ag-Ni/SBA-15 [17], Ag/SiO_2 [18], $Cu-Ni/SiO_2$ [19a], $Cu/ZnO/Al_2O_3$ [19b], Cu/TiO_2 [20], Cu/SiO_2-HZSM-5 [21], Cu/ZrO_2 [16], Cu/Al_2O_3 [16] and, Hydroxyapatite-supported Cu [22]. Other strategies for improving the stability and selectivity, like the use of monolithic Pd–Au–CuO_x/Cu-fiber catalyst with improved thermal conductivity of the support [15] and the functionalization of the Cu/SiO_2 catalysts by organo-silane compounds [3], were reported. However, Cu/SiO_2 catalysts are still the most studied ones due to the low density of acidic/basic sites on the SiO_2 support, limiting the formation of byproducts, even though stability is still an issue [12]. The deactivation of such catalysts was attributed to Cu sintering due to the weak interaction of Cu with SiO_2 [14,23] or to the poor SiO_2 thermal conductivity and generation of hotspots [15], Ostwald ripening of Cu induced by CO from MeOH dissociation [24,25] and poisoning [26], erosion of the Si support by the generation of silanes [27], pore-blocking by polymerization of methyl glycolate [28], and carbon deposition [29]. Several strategies were used to improve the stability of Cu/SiO_2 catalysts. Among these: doping with boron oxide [6,30], lanthanum oxide [23], Sn [29], ZrO_2, preparation of bimetallic catalysts like AuCu/SBA-15, the use of SiO_2 supports with nanosized pores [14]. Several preparation methods were proposed to improve the stability and selectivity of Cu/SiO_2 catalysts, like urea hydrolysis deposition precipitation [31], urea-assisted gelation [23], deposition-decomposition (DD) also known as Ammonia Evaporation [32], ammonium carbonate deposition precipitation [33] and, ionic exchange [34a]. Among these, the DD method allows obtaining an enhanced metal-support interaction, high Cu dispersion after controlled reduction [34b]. Therefore, the DD method was extensively studied for improving catalysts' stability and EG yields. More specifically, it has been optimized as a function of the temperature used during the DD procedure [35], the SiO_2 sol precursor dispersion [36], the order of addition of precursors [37], and the concentration of dextrin as a structural promoter in a modified version of the procedure [38].

Moreover, the extensive amounts of Cu^+ on the catalytic surface of DD catalysts are reported to work synergistically with metallic Cu for the DMO hydrogenation, as supported by XPS and TPR measurements [32]. More specifically, metallic Cu is believed to be the active site for the adsorption of H_2 and hydrogenation, while Cu^+ stabilizes methoxy and acyl intermediates and helps to polarize the C═O bond of DMO and MG [29,32]. Similar conclusions were also reached by kinetic modeling of the DMO hydrogenation on a Cu/SiO_2 catalyst prepared by the DD method, suggesting a dual-site Hougen-Watson mechanism with dissociative adsorption of both H_2 and esters and the dissociative adsorption of the DMO as the rate-determining step [39]. Therefore, a proper balance between surface Cu^+ and Cu sites is required. However, due to the dynamic change of the Cu oxidation state during the hydrogenation of esters [40], different views were reported regarding the optimal Cu^+/Cu ratio for improving the yield of EG [29], which can be related to the influence of the catalyst's preparation method, presence of promoters, reducing conditions [41], H_2/DMO ratio in the feed, working pressure and temperature, and aging of the catalyst. Moreover, few studies also reported the hydrogenation of diethyl oxalate to ethylene glycol as structure-sensitive [14].

Although many studies were undertaken to understand in depth the hydrogenation mechanism, even by using powerful characterization techniques, the structure of the active sites and the role of Cu^+ are still unknown. In addition, the formation of by-products like ethanol (EtOH) and 1,2-butanediol (1,2BD) by hydrodeoxygenation and Guerbet reactions [42–45a] was never analyzed in depth.

However, a reasonable hypothesis to explain the better performance of Cu based catalysts prepared by DD o similar procedures and to improve the understanding of the role of Cu^+ sites can be in extensive Cu ion exchange with the hydroxyls present on the SiO_2 support [45b], which after incomplete reduction, can effectively lead to a decreased exposition of acidic and basic sites from the support, limiting by-products formation and improving EG selectivity. In agreement, the pre-reduction of the catalyst and the employed testing conditions, in terms of H_2/DMO and H_2-GHSV, can largely influence the obtained EG selectivity.

Here, to test this hypothesis, the EG yield of a Cu/SiO_2 catalyst prepared by deposition-decomposition (DD) method was optimized at 200 °C and 25 barg, analyzing the formation of EtOH and 1,2BD, by modulating the initial reduction degree of the catalyst and the effect of the H_2/DMO and H_2-GHSV employed during the tests. The catalyst was pre-reduced a) in a 50% H_2/N_2 mixture at 200 °C, and in 100% H_2 at b) 200, c) 250, and d) 350 °C and tested at three different H_2/DMO and H_2-GHSV conditions. Then, using the most favorable reducing conditions, the effect of H_2-GHSV and H_2/DMO ratio was optimized in the range 1000–4000 h^{-1} and 30–200 mol/mol, respectively. After that, the time-on-stream stability of the catalyst was tested within the optimized conditions. To test the effect of the catalyst's reduction procedure on the metallic surface area, acidic and basic sites from the support, and the initial degree of reduction of the catalyst, the same catalyst was reduced in the above-reported conditions and measured by N_2O Chemisorption, FTIR and H_2-TPR, respectively. Finally, the possible structure of the active sites and Cu^+ role were rationalized to the obtained results and discussed.

2. Experimental

2.1. Catalyst preparation

The Cu/SiO_2 catalyst was prepared by deposition-decomposition (DD) method [46]. All the chemicals were used without further

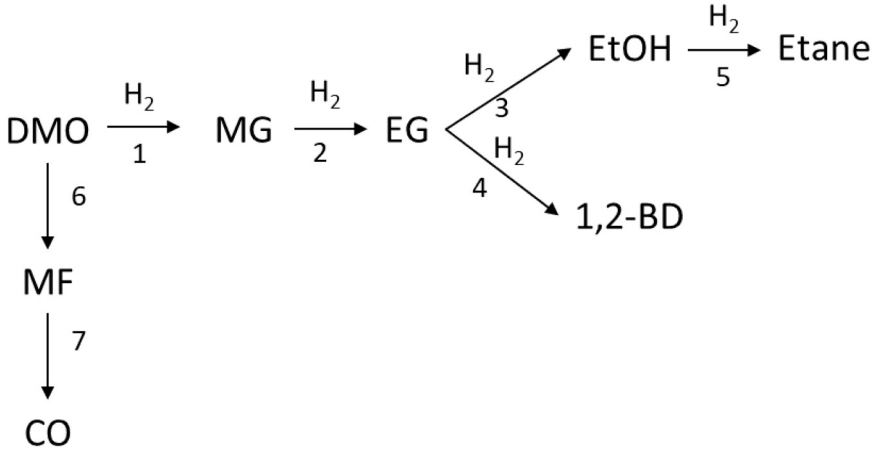

Scheme 1. Main reaction pathways.

purification. 15.25 g of $Cu(NO_3)_2.3H_2O$ (Carlo Erba Reagents, 475782) was mixed with 150 ml of deionized water and 46 ml of a 25% wt. NH_4OH (Sigma-Aldrich, 30501-M, $\geq$ 25% NH_3 basis). The resulting solution was stirred at 40 °C for 40 min. Then, 40 g of a 40 wt% colloidal SiO_2 (Alfa Aesar, 43110-A1, containing sodium as a counter-ion) were added, and the temperature was increased to 85 °C and kept constant for about 8 h. The final pH of the suspension was 6–7. The resulting suspension was separated by centrifugation and washed with 900 ml deionized water. The obtained solid was dried at 100 °C for 240 min and calcined at 450 °C (5 °C/min, 240 min).

2.2. Catalyst characterization

Cu loading of the prepared catalyst was estimated by atomic absorption spectroscopy analysis of the prepared catalysts. The Cu/SiO_2 catalyst was dissolved in a 47% wt. HF solution (Sigma-Aldrich, 339261) and diluted with deionized water. A Perkin-Elmer Analyst 200 at. absorption equipment measured the Cu concentration.

A Bruker D2 diffractometer (Bruker) recorded the x-ray diffraction pattern (XRD) of the calcined catalyst by employing the Ni-filtered Cu-kα radiation ($\lambda = 1.54178$ Å), in the 2θ range between 10° and 90° with a scanning rate of 0.04°/s and, operating at 30 kV and 10 mA.

An Autosorb IQ_3 sorption analyzer (Quantachrome), after evacuation at 300 °C for 240 min, measured the N_2 physisorption isotherms of the catalyst at −196 °C. The specific surface area (SA_{BET}) was calculated using the multipoint Brunauer Emmett Teller (BET) method in the range of 0.05–0.3 p/p°. The total pore volume was estimated at p/p° of 0.95. The pore size distribution was determined by the Barrett, Joyner & Halenda Method (BJH) using the N_2 desorption isotherm.

An Autochem II apparatus (Micromeritics) equipped with a TCD detector measured catalyst's temperature-programmed reduction (TPR) profiles and Cu metallic surface areas (Cu MSA).

The TPR profile of the fresh catalyst was measured on a 50 mg catalyst sample. Before the experiment, the catalyst was outgassed at 200 °C in He flow for 1 h and then cooled at room temperature. Finally, the gas flowing through the catalyst was switched to a 5% H_2/Ar mixture (40 ml/min), and the temperature increased to 900 °C (5 °C/min). Using the same conditions, the TPR profile of the catalyst pre-reduced in situ, in pure H_2, at 200 °C for 240 min (10 °C/min; H_2 GHSV 4000 h^{-1}) was investigated to get the reduction degree of the reduced catalyst.

The Cu MSA was measured after reducing the catalyst by pulse N_2O chemisorption at 90 °C [47], employing N_2 as a carrier [46]. The effect of the reduction procedure on the MSA was evaluated, reducing the catalyst: a) in pure hydrogen, at 200, 210, 250, and 350 °C; b) H_2/N_2 mixture at 200 °C; c) in 5% H_2/Ar at 350 °C. To mimic the pre-reduction procedures employed during the catalytic tests, the temperature ramp, time of permanence of the catalyst at the final temperature, and the H_2-GHSV of the reducing mixture were fixed at 10 °C/min, 240 min, and 4000 h^{-1}, respectively.

A CM12 transmission electron microscope (TEM, PHILIPS, point-to-point resolution, 3 Å), operating at 200 kV, imaged the catalyst. A small amount of the powdered catalyst was dispersed in 2-propanol (Sigma-Aldrich, I9516) using a sonic bath and then deposited on a Cu grid-supported holey carbon film.

A Vertex 70 FT-IR spectrometer, equipped with a mercury-cadmium-tellurium (MCT) liquid nitrogen cooled detector, and a commercial high-temperature vacuum diffused reflectance chamber with ZnSe windows, measured the diffuse reflectance infrared Fourier transform spectra (DRIFTS) of the prepared catalysts. The empty chamber was heated at 100 °C, and the instrumental background was recorded. Then, the catalyst was reduced in 100% H_2 at 200 °C or 350 °C (10 °C/min, 240 min), purged in N_2 flow, and cooled to 100 °C. Spectra were collected at 100 °C. DRIFTS spectra of the calcined sample were also recorded for comparison after degassing the sample at 200 °C under N_2 flow.

2.3. Testing and analysis

A PID Microactivity Effi (PID Eng. Tech / Micromeritics), equipped with two Hastelloy parallel tubular reactors (diameter: 91 mm), an HPLC pump and, two vapor-liquid separators, tested the activity of the prepared catalyst.

Typically, for each test, 0.85 g of fresh catalyst (16–25 mesh, 1.5 Ton; bed volume: 3 ml) were used.

Before each test, the catalyst was pre-reduced, using 1) 50% H_2/N_2 mixture and 2) in 100% H_2, with a temperature ramp of 10 °C/min at a) 200, b) 250 and, c) 350 °C for 240 min (final isotherm).

After reduction, the H_2 pressure was increased at 25 barg and the temperature set to 200 °C. Then a 20% wt. DMO/Methanol solution was fed to the reactor. The catalytic performance was optimized for the EG yield obtained at 200 °C and 25 barg, tuning the a) H_2 concentration during the catalyst pre-reduction procedure, b) pre-reduction temperature, c) H_2 GHSV, and d) H_2/DMO (Table 1). Each catalyst was tested at least 24–48 h, while the catalytic performance was compared only after steady-state conditions were achieved. The stability of the catalyst was studied for 60 h after choosing the optimal conditions for maximizing the EG yield.

Liquid samples were collected at room temperature by using a vapor-liquid separator at the reactor's exit. After the addition of n-heptane (internal standard), the collected samples were diluted in methanol and analyzed by using a GC-FID (TraceGC, Thermo), equipped with a split injector and an SPB-624 column (Supelco/Sigma Aldrich; code: 24255; phase: cyanopropylmethyl, phenylmethyl, polysiloxane; 30 m, 0.25 mm, 1.4 μm).

3. Results and discussion

3.1. Characterization

3.1.1. AAS and XRD

The Cu loading estimated by atomic absorption measurement of the prepared catalyst did not significantly differ from the designed loading

Table 1
Operating Conditions (Catalyst pre-reduced using a temperature ramp and isothermal time of 10 °C/min and 240 min, respectively; the amount of catalyst, testing temperature, and pressure fixed at 0.85 g, 200 °C, and 25 barg, respectively).

#	Reducing Mixture	Catalyst Pre-Reduction T (°C)	H_2 GHSV (h^{-1})	H_2/DMO (mol/mol)
1	50% H_2/N_2	200	2100	94
2				134
3	100% H_2	200	840	131.3
4			1040	33.2
5			1050	57
6				68.4
7			1080	168.8
8			1260	196.9
9			1460	65.2
10			1500	47.8
11				81.4
12				94
13			2100	67
14				94
15				114
16				134
17			2940	131.3
18			3000	94
19			4200	131.3
20		250	1050	68.4
21			2100	94
22				134
23		350	1050	68.4
24			2100	94
25				134

during the synthesis, indicating that most of the copper precursor was successfully deposited on the SiO_2 support.

The XRD pattern of the fresh calcined catalyst (Fig. 1) is in line with previously published results [33]. The XRD pattern shows mainly the presence of amorphous silica with a broad peak at 2θ of 21.04°, while the most intense peaks associated with the tenorite phase (CuO, COD, Ref. Num. 96-101-1195) are barely shown at 35.557° (1,1,1) and 38.763 (1,1,1). The latter, besides making unable the determination of the crystallite diameters of CuO_x species by the Scherrer equation, indicate that most of the Cu is present in the XRD-amorphous CuO or Cu phyllosilicate phase [33] as crystallites below 4 nm in diameter (XRD amorphous) or as a flat layer on the SiO_2 surface.

3.1.2. N_2 physisorption

The prepared catalyst presents type IV isotherm with an H3 hysteresis loop (Fig. 2), typical of mesoporous adsorbents in the presence of macropores [48]. The BET surface area is 387.9 m^2/g, the pore volume is 0.88 ml/g. The averaged mesopore diameter calculated by the volume pore size distribution by BJH is 16 nm. The large specific surface area of the calcined catalyst, with respect to the value reported by the manufacturer for the used colloidal silica (200 m^2/g), can be explained by the support's depolymerization and subsequent generation of small particles of phyllosilicate species during the DD procedure, due to the alkaline environment [49].

3.1.3. H_2-TPR

The H_2-TPR profile of the fresh calcined CuO/SiO_2 catalyst presents a single maximum at 207 °C (Fig. 3) and was deconvoluted in four overlapping Gaussian Peaks at 203 (P1), 219 (P2), 222 (P3) and a hardly visible peak at 320 °C (P4). The same catalyst (Cu/SiO_2), after pre-reduction in 100% H_2 at 200 °C (10 °C/min, 240 min) presents a convoluted peak at 90 °C and a rather flat peak at 326 °C. Its deconvolution resulted into four Gaussian peaks. Peaks P1–P3 present maxima below the P1 peak observed for the calcined catalyst, while the P4 was similar (Fig. 3, Inset). The CuO standard's H_2-TPR profile, reported as a reference, presents only a peak at 257 °C (RP) which was deconvoluted into two peaks at 254 (P1) and 266 °C (P2).

Peaks P1 and P2 in the reference CuO were related to the two-step reduction of CuO. Instead, in the case of the calcined CuO/SiO_2 catalyst, peaks P1 and P2 were assigned to bulk highly dispersed CuO nanoparticles [46], in agreement with the low temperature shift observed as compared with the reference CuO. The peak P3 was attributed to the presence of larger CuO particles while the peak P4 at 326 °C, although observed at the sensitivity limits of the measurements and at higher temperatures than the ones reported in other papers [50], was assigned to the presence of CuO_x species in close interaction with support e.g., by its -OH moieties or Cu phyllosilicate species [41]. The

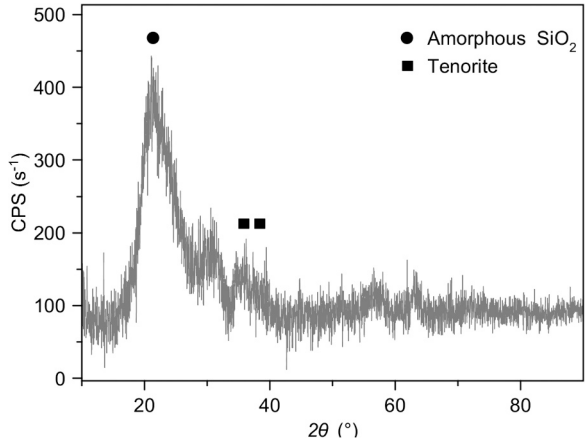

Fig. 1. XRD pattern of the Fresh Calcined Catalyst.

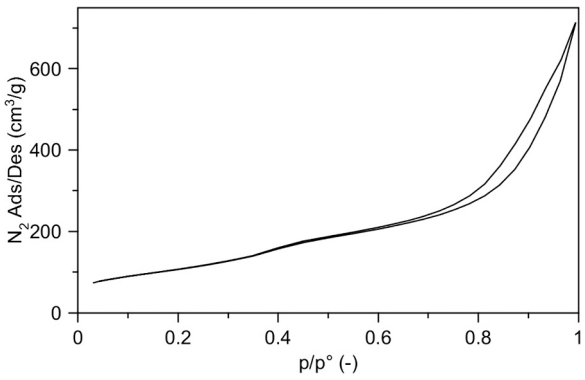

Fig. 2. N_2 adsorption isotherm at 77 K of the calcined catalyst.

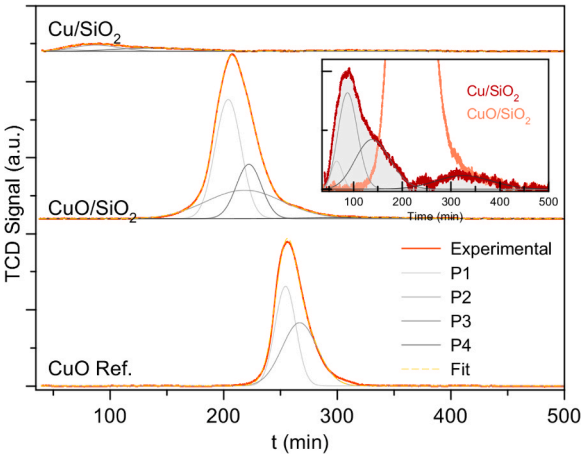

Fig. 3. TPR of the a) CuO reference standard, b) CuO/SiO_2 – fresh calcined catalyst, c) Cu/SiO_2 – fresh catalyst after reduction at 200 °C in 100% H_2 within the same conditions used for the tests (5% H_2/Ar, 3 °C/min, 240 min, 1.013 bar). In the inset the magnified superposition of the measured TPR spectra of the reduced Cu/SiO_2 catalyst and the CuO/SiO_2.

small peak at 90 °C observed for the reduced Cu/SiO_2 catalyst (200 °C, 100% H_2, 240 min), was associated to the incomplete reduction of Cu present as highly dispersed CuO, while the small peak at 326 °C was assigned to the hardly reducible Cu phyllosilicate species [41]. The total amount of oxidized species after reduction at 200 °C and atmospheric pressure accounted for 10% of the total hydrogen consumed in the reduction of the calcined CuO/SiO_2 catalyst, while the peak at 326 °C for less than 1%. The increased reduction degree of Cu/SiO_2 catalyst after increasing the catalyst's pre-reduction temperature within 200 and 250 °C for Cu/SiO_2 catalysts and its invariance above 250 °C was previously reported by Sun et. Al. by AES measurements [41]. Therefore, the H_2-TPR after pre-reducing the catalyst at 250 at 350 °C was not further investigated.

3.1.4. N_2O chemisorption

The Cu metallic surface area (MSA), as measured by N_2O chemisorption, after pre-reduction in 100% H_2 increased with increasing the temperature of the pre-reduction treatment between 200 and 250 °C, while slightly decreased at 350 °C (Fig. 4). Similar Cu MSA were obtained after pre-reduction at 350 °C in 5% H_2/He and 200 °C in 100% H_2, while it was doubled at 350 °C in 100% H_2.

The observed increase of the Cu MSA after pre-reducing the catalyst in 100% H_2 at 200–250 °C was related to highly dispersed CuO nanoparticles interacting with the support, in agreement with H_2-TPR measurements and previous reports [41]. The decreased Cu MSA observed after further increasing the catalyst's pre-reduction temperature at

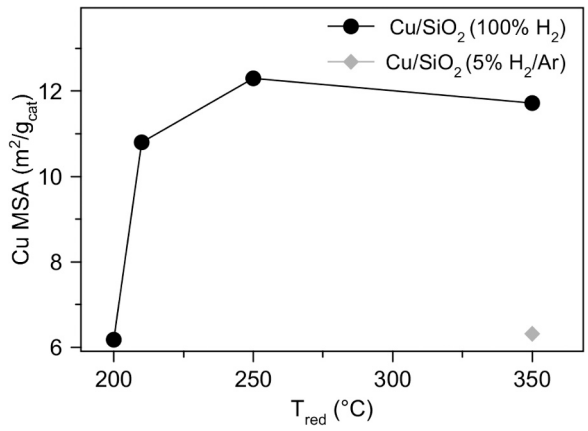

Fig. 4. Cu MSA measured by N_2O pulse chemisorption at 90 °C after reduction a) in pure H_2 and in b) 5% H_2/Ar mixture at the temperature indicated in the figure (the temperature ramp, the isothermal reduction step, and the pressure of H_2 were kept constant during the reduction, respectively at 10 °C/min, 240 min, 1.013 bar).

350 °C was linked to the decreased interaction of copper with the support and consequent sintering, as also observed by TEM micrograph analysis. The similar Cu MSA obtained after pre-reducing the catalyst at 350 °C in 5% H_2/Ar and 200 °C in 100% H_2 highlights a compensation effect between the temperature and hydrogen concentration during the pre-reduction procedure.

3.1.5. DRIFT

A large, convoluted band between 3200 and 3800 cm^{-1} in the —OH stretching region, and a band at 3615 cm^{-1} attributed to adsorbed water and OH- bound to highly dispersed of Cu ions on the support and found in the presence of Cu hydrosilicate or chrysocolla ($CuSiO_3 \cdot 2H_2O$) [49, 51] were observed in the case of the calcined catalyst (Fig. 5). After pre-reducing the catalyst at 200 °C in 100% H_2, while the intensity in the 3000–3300 cm^{-1} region increased, the 3615 cm^{-1} band did not change significantly, while a band at 3471 cm^{-1}, associated with terminal -OH SiO_2 surface slightly increased [31]. The intensity of such a band further increased after pre-reducing the catalyst at 350 °C in 100% H_2. At the same time, the bands within the 3200–3700 cm^{-1} region decreased.

The presence of the 3615 cm^{-1} band on the calcined catalyst and on the pre-reduced catalyst at 200 °C in 100% H_2 suggests the presence of large amounts of un-reduced copper interacting with the support. The decreased intensity of the latter band after pre-reducing the catalyst at 350 °C in 100% H_2 was related to the increased reduction degree of Cu

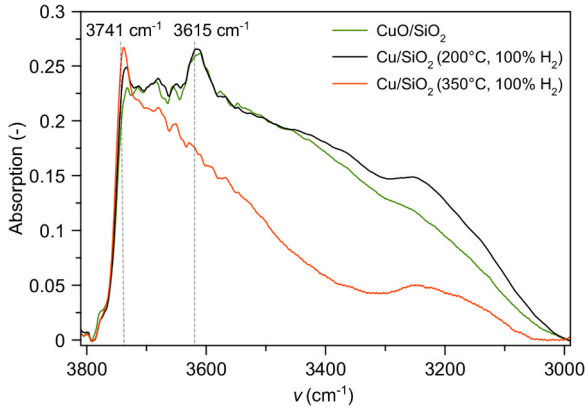

Fig. 5. DRIFTS of the fresh catalyst: as prepared (calcined) and after pre-reduction in 100% H_2 at 200 and 350 °C (ramp: 10 °C/min, isothermal time at the final temperature: 240 min, 1.013 bar).

and conversion of the Cu phyllosilicate phase. The increased intensity of the silanol band after pre-reducing the catalyst at 350 °C in 100% H_2 was attributed to the increased availability of the support's surface, freed from the interaction with Cu and thus to its acidic/basic sites [3]. The latter is in agreement with N_2O chemisorption and H_2-TPR measurements, indicating an increase in the Cu MSA with the catalyst's pre-reduction temperature between 200 and 250 °C, and a significant amount of Cu in the oxidized state after pre-reduction at 200 °C. The increased density of both Lewis acidic and basic sites as a consequence of the increasing Cu metallic surface and their relationship with the amount of formed Cu phyllosilicate, supported by FT-IR, NH_3-TPD, CO_2-TPD, and N_2O-H_2 redox titration measurements, was already reported for Cu/SiO_2 catalysts prepared by modulating the addition of precursors during the procedure [37]. Therefore, the increased silanol band after increasing the catalyst's pre-reduction temperature and the observed increase in the Cu MSA can be considered as descriptors indicating the increase of acidic and basic sites from the support.

3.1.6. TEM

The TEM micrographs of the catalyst after pre-reduction in 100% H_2 at 200 °C and 350 °C are shown in Fig. 6. The high density of vicinal Cu nanoparticles and the low contrast of Cu on the SiO_2 surface, related to the high Cu loading and its easy oxidation (18% wt, as measured by AAS) did not allow to estimate of the particle size distribution. After pre-reduction at 200 °C (Fig. 6a), Cu nanoparticles present the formation of a high density of vicinal hemispherical nanoparticles of about 10 nm, in agreement with the formation of an amorphous surface Cu phyllosilicate phase, evidenced by XRD measurement. After pre-reducing the catalyst at 350 °C (Fig. 6b), the observed Cu nanoparticles were more spherical and aggregated. The observed morphological change of Cu nanoparticles at 350 °C indicates a decreased metal-support interaction between Cu and SiO_2. In agreement with H_2-TPR, N_2O Chemisorption, and DRIFT measurements, a bimodal distribution of Cu nanoparticles is expected after pre-reducing the catalyst at 350 °C in 100% H_2.

3.2. Catalytic performance

3.2.1. Effect of the H_2 concentration during the catalyst pre-reduction procedure

The effect of H_2 concentration in the catalyst's pre-reduction procedure on the catalytic performance was tested by pre-reducing the catalyst at 200 °C (10 °C/min, 240 min), using 1) a 50% H_2/N_2 mixture and, 2) 100% H_2. Then the catalytic performance was tested using an H_2 GHSV of 2100 h^{-1} and H_2/DMO of a) 94 and b) 134 mol/mol (Table 1, conditions #1–2, 14, 16).

The DMO conversion was complete for all tested conditions. The MG yield (Fig. 7) was below 1% except at H_2/DMO of 94 mol/mol (7 ± 1.4%), after reduction in 100% H_2. The EG yield was about 80% in almost all the cases, while it decreased to 70 ± 3% after pre-reducing the catalyst in 50% H_2/N_2, operating at H_2/DMO of 134 mol/mol. The EtOH and 12-BD yields did not change significantly because of the different pre-reduction procedures. Instead, both the EtOH and 1,2-BD yields increased after increasing the H_2/DMO to 134 mol/mol. The DP yield (sum of non-analyzed reaction products) decreased after pre-reducing the catalyst in 100% H_2, while the operative H_2/DMO ratio did not significantly influence it. The best EG yield, and the lowest DP yields were obtained after pre-reducing the catalyst in 100% H_2.

The complete DMO conversion indicates that the DMO consumption rate is not affected by the H_2 concentration during pre-reduction at 200 °C. The latter behavior was also observed for MG, except the case of the pre-reduction treatment in 100% H_2 and H_2/DMO ratio of 94 mol/mol, where the MG yield slightly increases, leading to a decreased $Cu^{\delta+}$/Cu ratio and the imbalanced H_2 partial pressure. The enhanced EG yield, using the same pre-reduction treatment after increasing the H_2/DMO ratio to 134 mol/mol, was linked to the effect of a larger amount of H_2 on the catalytic surface, increasing the MG consumption rate. The DP

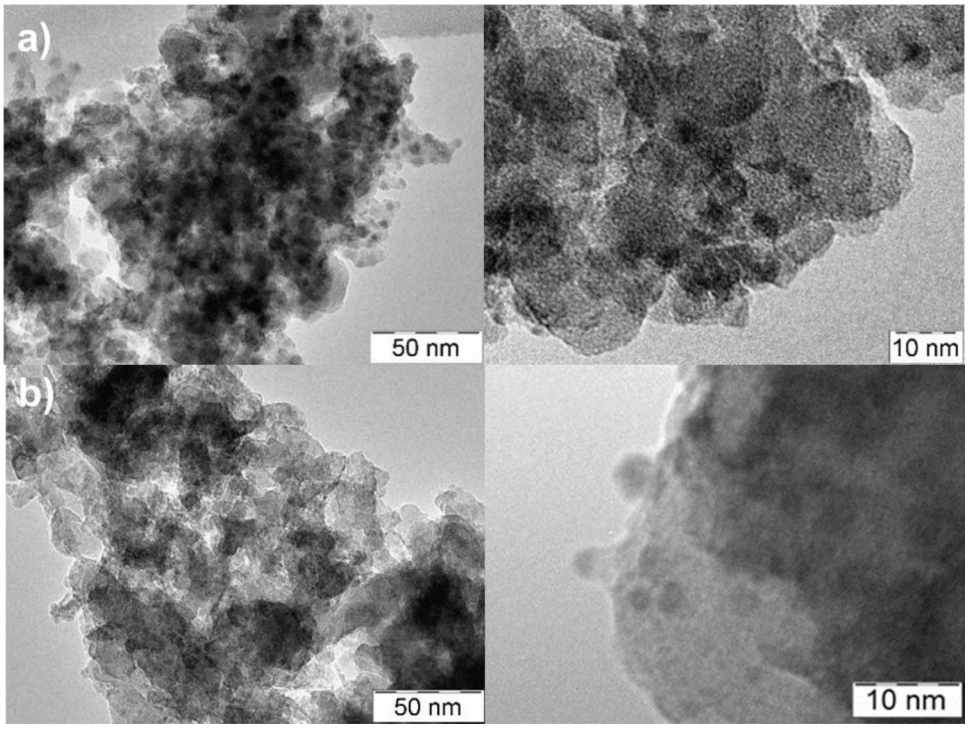

Fig. 6. TEM micrographs of the catalyst after reduction in pure H_2 a) at 200 °C and b) at 350 °C (the temperature ramp, the isothermal reduction step, and the pressure of H_2 were kept constant during the reduction, respectively at 10 °C/min, 240 min, 1.013 bar).

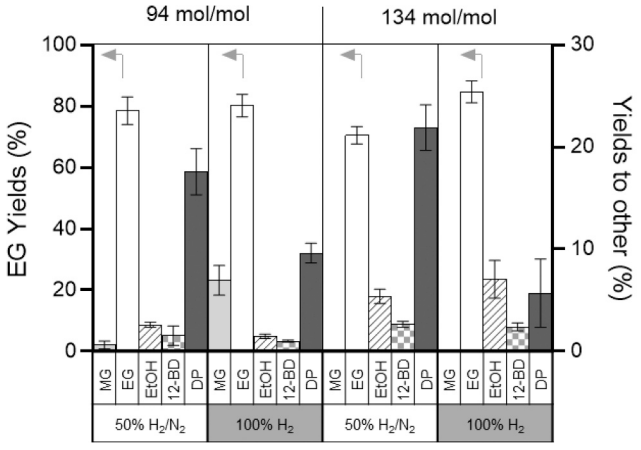

Fig. 7. Effect of the H_2 concentration in the catalyst reduction treatment on the product distribution operating with H_2/DMO of 94 and 134 mol/mol (Catalyst's pre-reduction at 200 °C, 10 °C/min for 240 min in 100% H_2 or 50% H_2/N_2 – Testing conditions: 200 °C, 25 barg, H_2 GHSV 2100 h^{-1}).

yields observed after pre-reducing the catalyst in 50% H_2/N_2 observed for both the analyzed H_2/DMO ratios were attributed to the decomposition of strongly chemisorbed DMO on $Cu^{\delta+}$ sites [41].

3.2.2. *Effect of the catalyst pre-reduction temperature*

The effect of catalyst's pre-reduction temperature on the catalytic performance was tested by pre-reducing the catalyst in 100% H_2, at a) 200 °C, b) 250 °C, c) 350 °C (10 °C/min, 240 min), using H_2 GHSV and H_2/DMO ratios, respectively, of 1) 1050 h^{-1}–68.4 mol/mol, 2) 2100 h^{-1}–94 mol/mol, 3) 2100 h^{-1}–134 mol/mol (Table 1, #6, 14, 16, 20–25).

Although the DMO conversion was complete in all the cases, the catalyst's pre-reduction temperature, the used H_2 GHSV, and H_2/DMO ratios affected the reaction's product distribution (Fig. 8). From the obtained results, the best EG yields (91%) were achieved after pre-reducing the catalyst at 200 °C, using an H_2/DMO and an H_2-GHSV of 68.4 mol/mol and 1050 h^{-1}, respectively (Fig. 8b). Moreover, at all the tested H_2-GHSV and H_2/DMO ratios, after increasing the catalyst's pre-reduction temperature from 200 °C to 350 °C in 100% H_2, the EG yield decreases significantly from 80% to 90% to 58–65%, while all the byproducts yield increase, accordingly. However, such trends are far from linear and significant deviations were found after pre-reducing the catalyst at 250 °C.

Such deviations, however, can be rationalized by considering the observed trends in the Cu-MSA with respect to the catalyst's pre-reduction temperature and assuming an increased influence of the testing conditions in terms of the employed H_2/DMO and H_2-GHSV. As previously shown in Fig. 4, a very steep increase of the Cu MSA was observed after pre-reducing the catalyst in 100% H_2 between 200 and 250 °C, while very subtle changes in the latter parameter were observed between 250 and 350 °C. Moreover, due to the introduction of DMO in the feed, the freshly reduced Cu gradually gets partially oxidated due to the decreased reducing potential of the feed with respect to pure H_2, used during the pre-reduction procedure. Therefore, the Cu MSA achieved after pre-reducing the catalyst at 200 °C and 350 °C, although slightly decreased introducing the feed, can be considered as almost invariant with respect to the used H_2/DMO and H_2-GHSV. After pre-reducing the catalyst at 250 °C, instead, even minor variations in the reducing potential of the feed can significantly affect the Cu MSA and, consequently, as shown by FTIR analysis of the pre-reduced catalysts, the availability of acidic and basic sites from the surface and the consequent products yields.

Although similar DMO conversion and EG yields trends as a function of the catalyst's pre-reduction temperature were reported by Sun et al. and attributed to the initial reduction state of Cu and to its role in promoting the adsorption of the esters and intermediates [41], only EG selectivity data were reported. Moreover, the complete DMO conversion observed in our conditions suggests that the catalyst's pre-reduction temperature does not influence the MG generation rate (Scheme 1, step 1). On the other hand, the increased 1,2-BD, EtOH, and DP yields

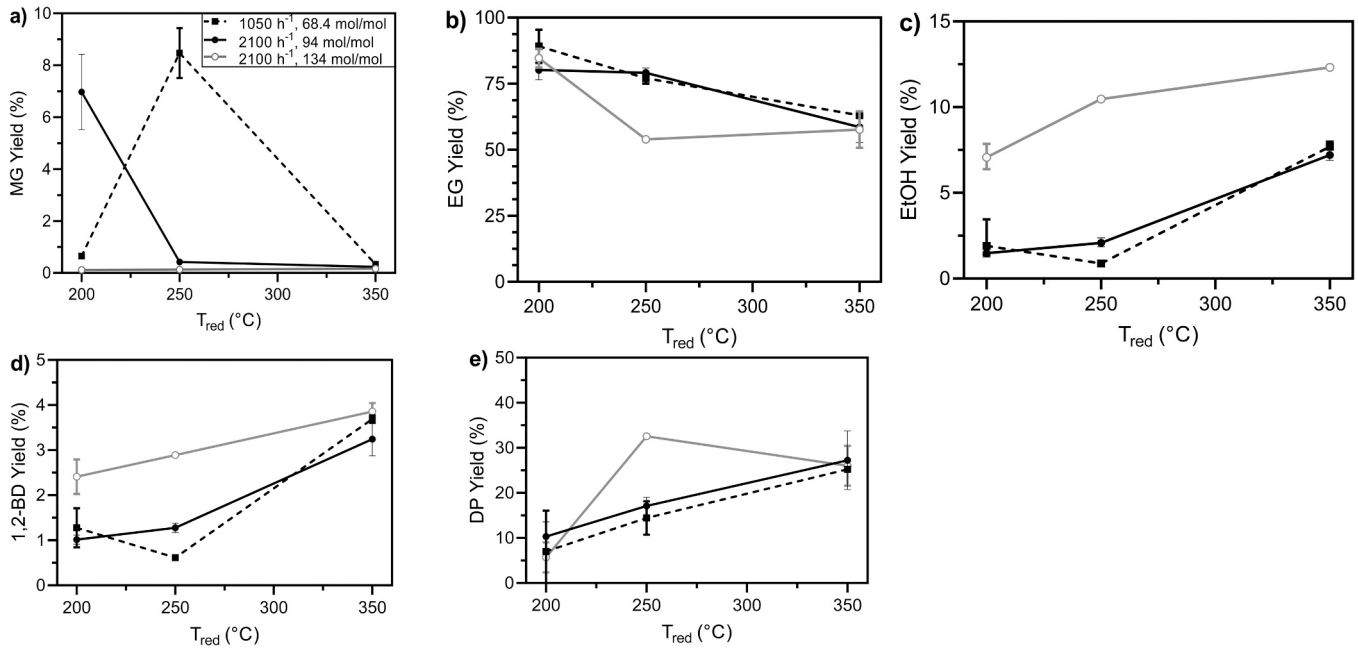

Fig. 8. Yields of a) MG, b) EG, c) EtOH, d) 1,2-BD and e) DP at 200 °C and 25 barg at three different H_2 GHSV – H_2/DMO conditions after reducing the catalyst in pure H_2 at 200, 250, and 350 °C in pure H_2 (ramp: 10 °C/min; final isothermal stage: 240 min, 1.013 bar).

after increasing the catalyst's pre-reduction temperature indicate an increase in the availability of vicinal acidic, basic, and metallic sites, leading to increased rates of hydrodeoxygenation and Guerbet reactions (steps 3 and 4, Scheme 1) [42–45]. Similar observations were also reported for the hydrogenation of ethyl acetate to ethanol, using Cu/SiO_2 catalysts as the function of Cu dispersions and the related density of Lewis acidic and basic sites, indicating an increase in the selectivity to ethane as a byproduct with increasing the Cu dispersion and the density of acidic/basic sites [37]. Therefore, it is possible to conclude that the role of Cu^+ sites in the DMO hydrogenation to EG is not just promoting the adsorption of the esters and intermediates but also mitigating the density of acidic and basic sites vicinal to metallic Cu nanoparticles.

3.2.3. Optimization of H_2/DMO and H_2 GHSV

After reducing the catalyst in 100% H_2 at 200 °C, operating at 200 °C and 25 barg, the catalytic performance was optimized modulating the H_2 GHSV and H_2/DMO in the range 840–4200 h^{-1} and 33–196 mol/mol, respectively (Table 1, #3–19).

The dimethyl oxalate (DMO) conversion (Fig. 9a) was complete (98%−100%) in almost all the analyzed conditions, while it decreased to 82–92% when the H_2/DMO was below 57 mol/mol. Reaction products were distributed in three distinct H_2 GHSV – H_2/DMO zones labeled as α, β, and γ (Fig. 9b–f). Operating with H_2 GHSV between 1000 and 3000 h^{-1} and low H_2/DMO values (α zone), the MG yield was between 27% and 54% (Fig. 9b), while the EG yield was between 15% and 65% (Fig. 9c). Operating with H_2/DMO and H_2 GHSV values of 54–131 mol/mol and 1050–2100 h^{-1} (β zone), the MG yields decreased between 0% and 7%, and EG yields between 71% and 86% were achieved. Operating at H_2/DMO > 140, within the γ zone, the EG yields decreased below 67%. The best EG yields of about 86% were observed at H_2 GHSV and H_2/DMO ratio of 1050 h^{-1} and 57–68.4 mol/mol. The main byproducts of the reaction were, in order of importance, DP > EtOH > 1,2-BD. Byproducts yields were low operating within the α zone, intermediate in the β zone, and large within the γ zone, where the most significant byproducts yields were obtained. Large DP yields were also observed operating at H_2/DMO and H_2 GHSV of 33.2 mol/mol and 1040 h^{-1}, respectively.

The observed trends are in line with the complex reaction kinetics (Scheme 1). The catalytic hydrogenation of MG (step 2) and the over-hydrogenation of EG to EtOH (step 3) are the most critical steps to be optimized. All the analyzed steps are dependent on the H_2 partial pressure. In addition, the high H_2/DMO ratio needed for converting DMO and MG is supported by the slow chemisorption of H_2 on the Cu surface [52]. Among the analyzed byproducts, after increasing the H_2/DMO ratio, the EtOH yield increased more than 1,2-BD. The increased yields of EtOH and 1,2-BD observed at low H_2-GHSV, and high H_2/DMO can be related to a purely kinetic phenomenon. However, after reducing the catalyst at 200 °C in 100% H_2, the operating Cu MSA and density of acidic/basic sites can still change due to the different H_2/DMO related reducing potential of the feed. Therefore, the increased Cu MSA and related increase in density of acidic/basic sites because of the increased H_2/DMO could also be at the origin of the observed increase in the EtOH and 1,2-BD yields. The high DP yields achieved at low H_2-GHSV, after increasing the H_2/DMO ratio, suggest the over hydrogenation of EtOH to ethane [45] (Scheme 1, steps 3 and 5) and were explained using the previously reported hypothesis. Conversely, the high DP yields observed at 1040 h^{-1} and H_2/DMO of 33.2 mol/mol suggest the presence of a decomposition route for DMO [45] (Scheme 1, steps 6 and 7) due to the increased Cu^+/Cu achieved operating at low H_2/DMO ratio. In agreement with the above-reported reaction pathways, the best EG yields were achieved operating with an H_2-GHSV of 1050 h^{-1} and H_2/DMO ratios of 57 and 68.4 mol/mol.

3.2.4. Time stability of the catalyst

The time-onstream catalyst's stability was studied for 60 h after the catalyst's pre-reduction at 200 °C in 100% H_2, operating at 1050 h^{-1} and 68.4 mol/mol, where the best EG yields were achieved (Table 1, #6).

In these conditions, while the MG yield was stable below 1%, two reaction regions were observed (Figs. 10–12): a) an initial induction time, lasting about 20 h, and b) a steady-state region, between 20 and 60 h, in agreement with Zheng and He et al. [6,26]. During the initial induction period, both the DMO conversion and EG yield increased (Fig. 10). The DMO conversion was complete and steady-state after 10 h, while the EG yield increased from 56% to 91% and was constant only after 20 h. Conversely, the yields to EtOH, 1,2-BD, and DP decreased continuously during time-on-stream (Figs. 11 and 12).

The observed induction period is typical for Cu/SiO_2 catalysts and is

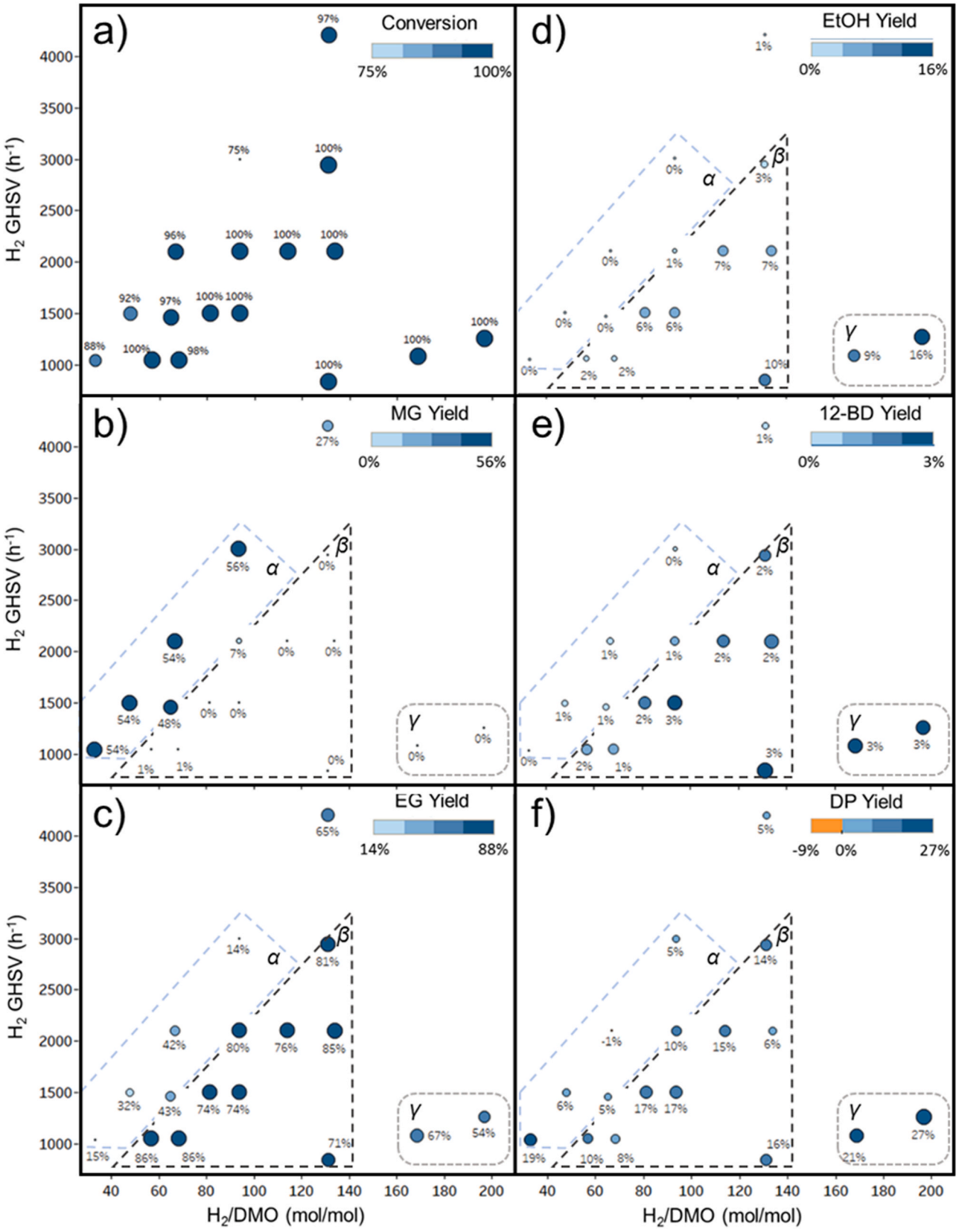

Fig. 9. Effect of H_2 GHSV (h^{-1}) and H_2/DMO (mol/mol) on the a) DMO Conversion and Yields of b) MG, c) EG, d) EtOH, e) 1,2-BD, and f) DP products (operating conditions: 200 °C, 25 barg; catalyst pre-reduced at 200 °C in H_2 at 200 °C, 10 °C/min, 1.013 bar for 240 min; color scales and points size are proportional to conversion and yields). (For interpretation of the references to color in this figure legend, the reader is referred to the web version of this article.)

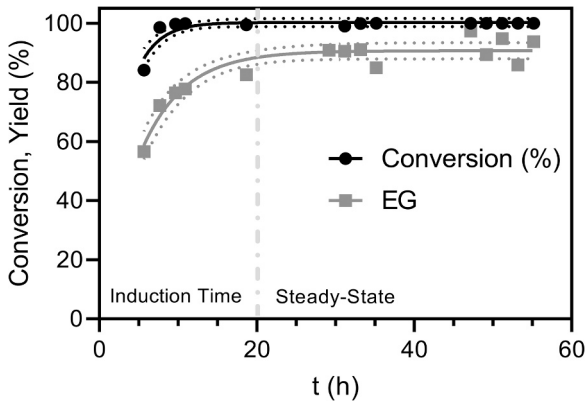

Fig. 10. Stability test: Effect of time (h) on DMO conversion and EG selectivity at 200 °C, 25 barg (H_2/DMO 68.3 mol/mol; GHSV 1050 h^{-1}; catalyst pre-reduced at 200 °C in H_2 at 200 °C, 10 °C/min, 1.013 bar for 240 min; interpolating lines: $y = p\bullet(1 - e^{-kt})$; 95% C.I.).

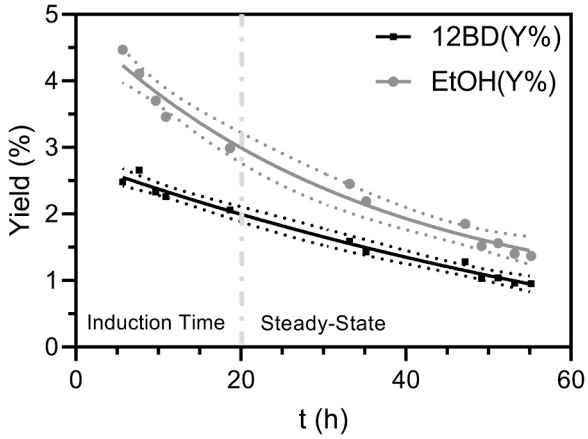

Fig. 11. TEM Stability test: Effect of time (h) on EtOH and 12-BD at 200 °C, 25 barg (H_2/DMO 68.3 mol/mol; GHSV 1050 h^{-1}; catalyst pre-reduced at 200 °C in H_2 at 200 °C, 10 °C/min, 1.013 bar for 240 min; interpolating lines: $y = p\bullet(-1 + e^{-kt})$; 95% C.I.).

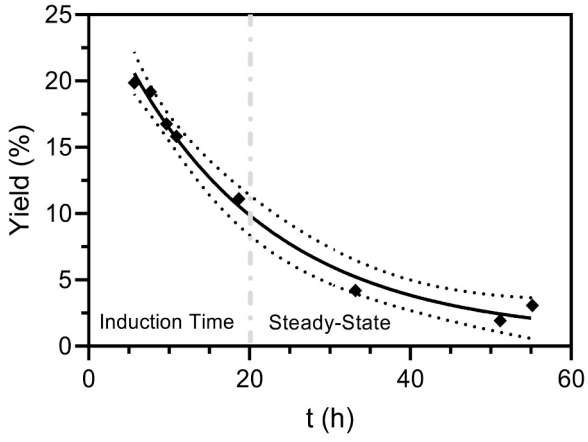

Fig. 12. Stability test: Effect of time (h) on HDP at 200 °C, 25 barg (H_2/DMO 68.3 mol/mol; GHSV 1050 h^{-1}; catalyst pre-reduced at 200 °C in H_2 at 200 °C, 10 °C/min, 1.013 bar for 240 min; interpolating line: $y = p\bullet(-1 + e^{-kt})$; 95% C.I.).

related to the slow oxidation of copper after introducing dimethyl oxalate, a mild oxidizing species, which decrease the reduction potential of the inlet stream [6,25,40]. As previously shown, the redox dynamics in Cu/SiO_2 catalysts in the hydrodeoxygenation of DMO is intimately related to the dynamic expression of acidity and basicity by the support. Therefore, the observed increase of the DMO conversion during the induction period and the decreased byproducts yield over time were related to the slow oxidation and spreading of highly dispersed Cu nanoparticles, increasing the metal-support interface, and leading to an increase of the DMO chemisorption and its hydrogenation rate to MG and EG. Such a behavior has been previously reported on Pd/Al_2O_3 catalysts after calcination [53,54] and could effectively decrease the density of vicinal metallic and acidic/basic sites and the rates of Guerbet and hydrodeoxygenation routes (Scheme 2). Moreover, the sites at the interface between metallic and oxidic Cu interface can be the main ones for the selective DMO and MG hydrogenation to EG. In line with the dynamic redox behavior of the Cu surface, a dependence of the Cu^+/Cu and the density of vicinal acidic and basic sites with respect to the employed H_2/DMO ratio is expected. Therefore, the formation of byproducts is not a purely kinetic phenomenon, and the surface concentration of active sites cannot be considered invariant. It follows that it is not possible to confine the role of Cu^+ only as a preferential site for DMO and MG chemisorption [32,55] but also as a spacer for avoiding the formation of unselective multifunctional vicinal sites. In agreement, very interesting results were reported by encapsulating Cu_2O nanoparticles in mesoporous silica, where an enhanced Cu-support interface was obtained [56].

4. Conclusions

The catalytic hydrogenation of DMO to EG was investigated in a fixed-bed reactor for the Cu/SiO_2 catalyst prepared by deposition-decomposition (DD) method using ammonium hydroxide. The prepared catalyst was tested at 200 °C and 25 barg, the best catalytic performance in terms of EG yield was achieved after reducing the catalyst at 200 °C in pure H_2. This treatment leads to an optimal tradeoff between the achieved metallic surface area of copper and the concentration of vicinal acidic/basic hydroxyls and metallic sites, minimizing the formation of over-hydrogenated byproducts. The experimental conditions were further optimized with respect to the H_2 GHSV and H_2/DMO ratio, operating in the range 1000–4000 h^{-1} and 40–200 mol/mol, while keeping the operating temperature and pressure fixed at 200 °C and 25 barg, respectively. The obtained results indicate an optimum catalyst performance with a GHSV of 1050 h^{-1} and H_2/DMO of 68. A 92% yield was achieved operating in optimized conditions for a time-on-stream of 50 h. Testing the catalyst time-on-stream stability, the conversion and ethylene glycol productivity increased during the first 20 h and were stable for the remaining time. Conversely, a decreasing yield of over hydrogenated byproducts was found over the investigated time-on-stream, which was related to the slow oxidation of Cu at the metal-support interface. The presence of Cu^+ sites on the borders of Cu nanoparticles at the metal-support interface was shown to be the key optimization factor for improving dimethyl oxalate conversion, increasing the EG yield and decreasing the yield of over hydrogenated byproducts.

Moreover, increasing the concentration of unreduced Cu can lead to an insufficient surface concentration of H_2 and DMO decomposition, as shown by comparing the EG and DP yields after pre-reducing the catalyst at 200 °C in 50% H_2/N_2 and 100% H_2. In comparison, the Cu over-reduction at temperature higher than 200 °C leads to vicinal metallic and acidic/basic sites.

The present results offer a new and cost-effective way for the optimization of the catalytic performance of Cu/SiO_2 catalysts, potentially improving their durability and opening new ways of improving the development of new catalysts and their industrialization.

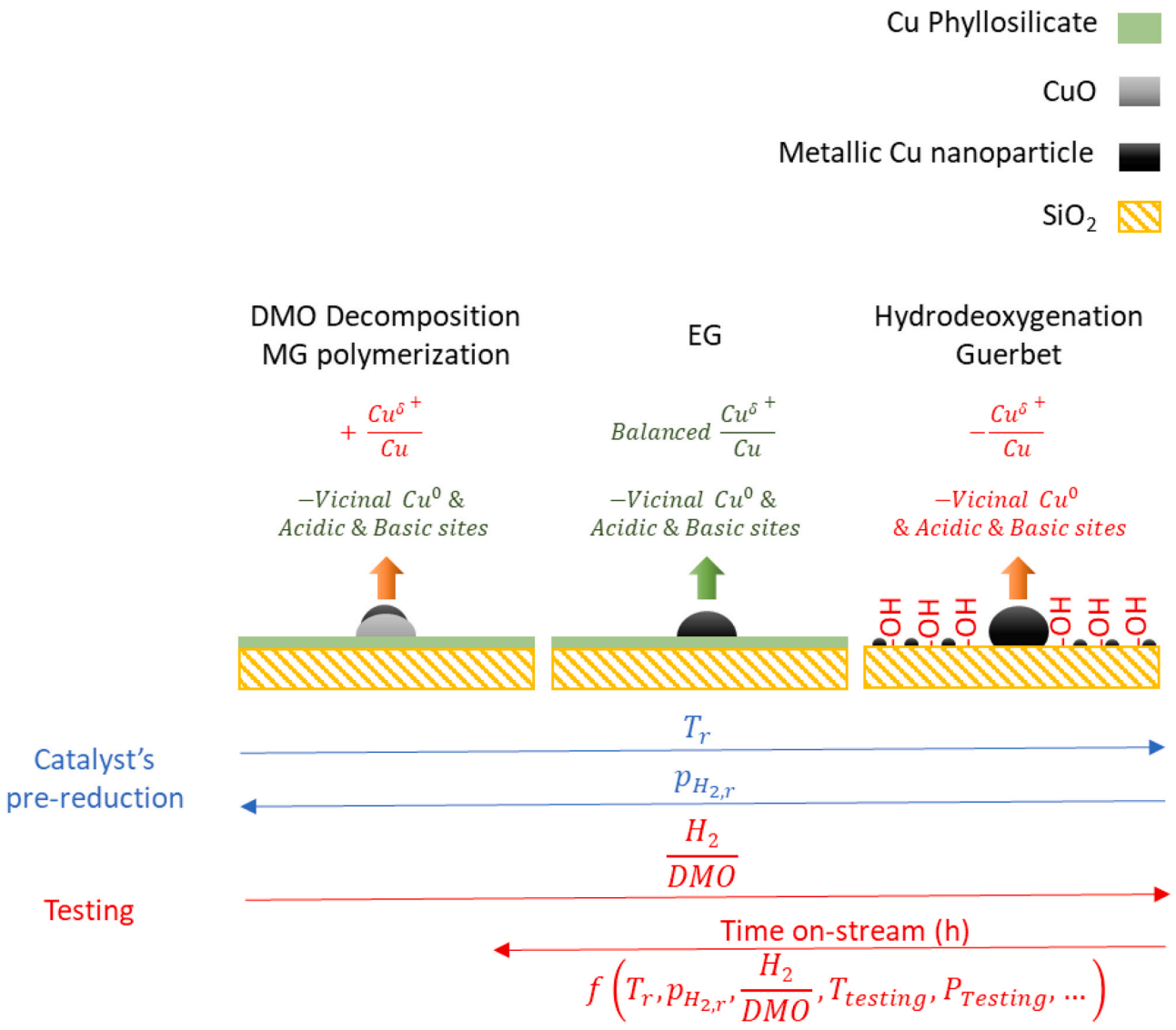

Scheme 2. Dynamic state of the catalytic surface.

Declaration of Competing Interest

The authors declare that they have no known competing financial interests or personal relationships that could have appeared to influence the work reported in this paper.

Acknowledgments

This project has received funding from the European Union's Horizon 2020 research and innovation program under grant agreement No 767798 (OCEAN).

References

[1] Ethylene glycol production capacity globally 2024 | Statista, n.d. ⟨https://www.statista.com/statistics/1067418/global-ethylene-glycol-production-capacity/⟩ (Accessed 2 June 2021).
[2] H. Yue, Y. Zhao, X. Ma, J. Gong, Ethylene glycol: properties, synthesis, and applications, Chem. Soc. Rev. 41 (2012) 4218–4244, https://doi.org/10.1039/c2cs15359a.
[3] M. Wang, D. Yao, A. Li, Y. Yang, J. Lv, S. Huang, Y. Wang, X. Ma, Enhanced selectivity and stability of Cu/SiO_2 catalysts for dimethyl oxalate hydrogenation to ethylene glycol by using silane coupling agents for surface modification, Ind. Eng. Chem. Res. 59 (2020) 9414–9422, https://doi.org/10.1021/acs.iecr.0c00789.
[4] B.Y. Yu, I.L. Chien, Design and optimization of dimethyl oxalate (DMO) hydrogenation process to produce ethylene glycol (EG), Chem. Eng. Res. Des. 121 (2017) 173–190, https://doi.org/10.1016/j.cherd.2017.03.012.
[5] X. Gao, Y. Zhao, S. Wang, Y. Yin, B. Wang, X. Ma, A Pd-Fe/α-Al_2O_3/cordierite monolithic catalyst for CO coupling to oxalate, Chem. Eng. Sci. 66 (2011) 3513–3522, https://doi.org/10.1016/j.ces.2011.04.012.
[6] Z. He, H. Lin, P. He, Y. Yuan, Effect of boric oxide doping on the stability and activity of a Cu-SiO_2 catalyst for vapor-phase hydrogenation of dimethyl oxalate to ethylene glycol, J. Catal. 277 (2011) 54–63, https://doi.org/10.1016/j.jcat.2010.10.010.
[7] U. Matteoli, G. Menchi, M. Bianchi, F. Piacenti, Homogeneous catalytic hydrogenation dicarboxylic acid esters. II, J. Organomet. Chem. 299 (1986) 233–238, https://doi.org/10.1016/0022-328X(86)82019-8.
[8] U. Matteoli, M. Bianchi, G. Menchi, P. Frediani, F. Piacenti, Hydrogenation of dimethyl oxalate in the presence of ruthenium carbonyl carboxylates: ethylene glycol formation, J. Mol. Catal. 29 (1985) 269–270, https://doi.org/10.1016/0304-5102(85)87009-7.
[9] U. Matteoli, G. Menchi, M. Bianchi, F. Piacenti, Homogeneous catalytic hydrogenation of the esters of bicarboxylic acids, J. Mol. Catal. 44 (1988) 347–355, https://doi.org/10.1016/0304-5102(88)80020-8.
[10] U. Matteoli, G. Menchi, M. Bianchi, F. Piacenti, Selective reduction of dimethyl oxalate by ruthenium carbonyl carboxylates in homogeneous phase Part IV, J. Mol. Catal. 64 (1991) 257–267, https://doi.org/10.1016/0304-5102(91)85135-O.
[11] H.T. Teunissen, C.J. Elsevier, Ruthenium catalysed hydrogenation of dimethyl oxalate to ethylene glycol, Chem. Commun. (1997) 667–668, https://doi.org/10.1039/a700862g.
[12] D.S. Brands, E.K. Poels, A. Bliek, Ester hydrogenolysis over promoted Cu/SiO_2 catalysts, Appl. Catal. A Gen. 184 (1999) 279–289, https://doi.org/10.1016/S0926-860X(99)00106-4.

[13] X. Kong, C. Ma, J. Zhang, J. Sun, J. Chen, K. Liu, Effect of leaching temperature on structure and performance of Raney Cu catalysts for hydrogenation of dimethyl oxalate, Appl. Catal. A Gen. 509 (2016) 153–160, https://doi.org/10.1016/j.apcata.2015.10.029.

[14] J. Ding, J. Zhang, C. Zhang, K. Liu, H. Xiao, F. Kong, J. Chen, Hydrogenation of diethyl oxalate over Cu/SiO_2 catalyst with enhanced activity and stability: contribution of the spatial restriction by varied pores of support, Appl. Catal. A Gen. 508 (2015) 68–79, https://doi.org/10.1016/j.apcata.2015.10.006.

[15] L. Han, L. Zhang, G. Zhao, Y. Chen, Q. Zhang, R. Chai, Y. Liu, Y. Lu, Copper-fiber-structured Pd-Au-CuO x: preparation and catalytic performance in the vapor-phase hydrogenation of dimethyl oxalate to ethylene glycol, ChemCatChem 8 (2016) 1065–1073, https://doi.org/10.1002/cctc.201501415.

[16] Y. Zhu, Y. Zhu, G. Ding, S. Zhu, H. Zheng, Y. Li, Highly selective synthesis of ethylene glycol and ethanol via hydrogenation of dimethyl oxalate on Cu catalysts: influence of support, Appl. Catal. A Gen. 468 (2013) 296–304, https://doi.org/10.1016/j.apcata.2013.09.019.

[17] M.M.J. Li, L. Ye, J. Zheng, H. Fang, A. Kroner, Y. Yuan, S.C.E. Tsang, Surfactant-free nickel-silver core@shell nanoparticles in mesoporous SBA-15 for chemoselective hydrogenation of dimethyl oxalate, Chem. Commun. 52 (2016) 2569–2572, https://doi.org/10.1039/c5cc09827k.

[18] A. Yin, X. Guo, W. Dai, K. Fan, High activity and selectivity of Ag/SiO_2 catalyst for hydrogenation of dimethyl oxalate, Chem. Commun. 46 (2010) 4348–4350, https://doi.org/10.1039/c0cc00581a.

[19] a) J. Zhu, Y. Ye, Y. Tang, L. Chen, K. Tang, Efficient hydrogenation of dimethyl oxalate to ethylene glycol via nickel stabilized copper catalysts, RSC Adv. 6 (2016) 111415–111420, https://doi.org/10.1039/C6RA23474G;
b) C. Wen, F. Li, Y. Cui, W.L. Dai, K. Fan, Investigation of the structural evolution and catalytic performance of the CuZnAl catalysts in the hydrogenation of dimethyl oxalate to ethylene glycol, Catal. Today 233 (2014) 117–126, https://doi.org/10.1016/j.cattod.2013.10.075.

[20] B. Wang, Y. Cui, C. Wen, X. Chen, Y. Dong, W.L. Dai, Role of copper content and calcination temperature in the structural evolution and catalytic performance of Cu/P25 catalysts in the selective hydrogenation of dimethyl oxalate, Appl. Catal. A Gen. 509 (2016) 66–74, https://doi.org/10.1016/j.apcata.2015.10.022.

[21] H. Lin, X. Zheng, Z. He, J. Zheng, X. Duan, Y. Yuan, Cu/SiO_2 hybrid catalysts containing HZSM-5 with enhanced activity and stability for selective hydrogenation of dimethyl oxalate to ethylene glycol, Appl. Catal. A Gen. 445–446 (2012) 287–296, https://doi.org/10.1016/j.apcata.2012.08.025.

[22] C. Wen, Y. Cui, X. Chen, B. Zong, W.L. Dai, Reaction temperature controlled selective hydrogenation of dimethyl oxalate to methyl glycolate and ethylene glycol over copper-hydroxyapatite catalysts, Appl. Catal. B Environ. 162 (2015) 483–493, https://doi.org/10.1016/j.apcatb.2014.07.023.

[23] X. Zheng, H. Lin, J. Zheng, X. Duan, Y. Yuan, Lanthanum oxide-modified Cu/SiO_2 as a high-performance catalyst for chemoselective hydrogenation of dimethyl oxalate to ethylene glycol, ACS Catal. 3 (2013) 2738–2749, https://doi.org/10.1021/cs400574v.

[24] J. Lin, X. Zhao, Y. Cui, H. Zhang, D. Liao, Effect of feedstock solvent on the stability of Cu/SiO_2 catalyst for vapor-phase hydrogenation of dimethyl oxalate to ethylene glycol, Chem. Commun. 48 (2012) 1177–1179, https://doi.org/10.1039/c1cc15783c.

[25] R.-P. Ye, L. Lin, Q. Li, Z. Zhou, T. Wang, C.K. Russell, H. Adidharma, Z. Xu, Y.-G. Yao, M. Fan, Recent progress in improving the stability of copper-based catalysts for hydrogenation of carbon–oxygen bonds, Catal. Sci. Technol. 8 (2018) 3428–3449, https://doi.org/10.1039/C8CY00608C.

[26] J. Zheng, J. Zhou, H. Lin, X. Duan, C.T. Williams, Y. Yuan, CO-mediated deactivation mechanism of SiO_2-supported copper catalysts during dimethyl oxalate hydrogenation to ethylene glycol, J. Phys. Chem. C 119 (2015) 13758–13766, https://doi.org/10.1021/acs.jpcc.5b03569.

[27] C. Wen, Y. Cui, W.-L. Dai, S. Xie, K. Fan, Solvent feedstock effect: the insights into the deactivation mechanism of Cu/SiO_2 catalysts for hydrogenation of dimethyl oxalate to ethylene glycol, Chem. Commun. 49 (2013) 5195–5197, https://doi.org/10.1039/c3cc40570b.

[28] D.J. Thomas, J.T. Wehrli, M.S. Wainwright, D.L. Trimm, N.W. Cant, Hydrogenolysis of diethyl oxalate over copper-based catalysts, Appl. Catal. A, Gen. 86 (1992) 101–114, https://doi.org/10.1016/0926-860X(92)85141-W.

[29] C. Zhang, D. Wang, B. Dai, Promotive effect of Sn^{2+} on Cu^0/Cu^+ ratio and stability evolution of Cu/SiO_2 catalyst in the hydrogenation of dimethyl oxalate, Catalysts 7 (2017) 122, https://doi.org/10.3390/catal7040122.

[30] S. Zhao, H. Yue, Y. Zhao, B. Wang, Y. Geng, J. Lv, S. Wang, J. Gong, X. Ma, Chemoselective synthesis of ethanol via hydrogenation of dimethyl oxalate on Cu/SiO_2: enhanced stability with boron dopant, J. Catal. 297 (2013) 142–150, https://doi.org/10.1016/j.jcat.2012.10.004.

[31] S. Hui, B. Zhang, S. Zhang, W. Li, In situ IR study of dimethyl oxalate hydrogenation to ethylene glycol over Cu/SiO_2 catalyst, J. Nat. Gas Chem. 21 (2012) 753–758, https://doi.org/10.1016/S1003-9953(11)60428-3.

[32] L.F. Chen, P.J. Guo, M.H. Qiao, S.R. Yan, H.X. Li, W. Shen, H.L. Xu, K.N. Fan, Cu/SiO_2 catalysts prepared by the ammonia-evaporation method: texture, structure, and catalytic performance in hydrogenation of dimethyl oxalate to ethylene glycol, J. Catal. 257 (2008) 172–180, https://doi.org/10.1016/j.jcat.2008.04.021.

[33] J. Ding, T. Popa, J. Tang, K.A.M. Gasem, M. Fan, Q. Zhong, Highly selective and stable Cu/SiO_2 catalysts prepared with a green method for hydrogenation of diethyl oxalate into ethylene glycol, Appl. Catal. B Environ. 209 (2017) 530–542, https://doi.org/10.1016/j.apcatb.2017.02.072.

[34] a) A. Yin, X. Guo, K. Fan, W.L. Dai, Ion-exchange temperature effect on Cu/HMS catalysts for the hydrogenation of dimethyl oxalate to ethylene glycol, ChemCatChem 2 (2010) 206–213, https://doi.org/10.1002/cctc.200900244;
b) Z. Bian, S. Kawi, Preparation, characterization and catalytic application of phyllosilicate: a review, Catal. Today (2018), https://doi.org/10.1016/j.cattod.2018.12.030.

[35] L. Chen, P. Guo, M. Qiao, S. Yan, H. Li, W. Shen, H. Xu, K. Fan, Cu/SiO_2 catalysts prepared by the ammonia-evaporation method: texture, structure, and catalytic performance in hydrogenation of dimethyl oxalate to ethylene glycol, J. Catal. 257 (2008) 172–180, https://doi.org/10.1016/j.jcat.2008.04.021.

[36] C. Zhang, D. Wang, M. Zhu, F. Yu, B. Dai, Effect of different nano-sized silica sols as supports on the structure and properties of Cu/SiO_2 for hydrogenation of dimethyl oxalate, Catalysts 7 (2017) 75, https://doi.org/10.3390/catal7030075.

[37] Z. Chen, J. Zhang, M. Abbas, Y. Xue, J. Sun, K. Liu, J. Chen, Effect of configuration addition of precursors on structure and catalysis of Cu/SiO_2 catalysts prepared by ammonia evaporation-hydrothermal method, Ind. Eng. Chem. Res. 56 (2017) 9285–9292, https://doi.org/10.1021/acs.iecr.7b02034.

[38] R. Ye, L. Lin, J. Yang, M. Sun, F. Li, B. Li, Y. Yao, A new low-cost and effective method for enhancing the catalytic performance of Cu–SiO_2 catalysts for the synthesis of ethylene glycol via the vapor-phase hydrogenation of dimethyl oxalate by coating the catalysts with dextrin, J. Catal. 350 (2017) 122–132, https://doi.org/10.1016/j.jcat.2017.02.018.

[39] S. Li, Y. Wang, J. Zhang, S. Wang, Y. Xu, Y. Zhao, X. Ma, Kinetics study of hydrogenation of dimethyl oxalate over Cu/SiO_2 catalyst, Ind. Eng. Chem. Res. 54 (2015) 1243–1250, https://doi.org/10.1021/ie5043038.

[40] X. Ma, Z. Yang, X. Liu, X. Tan, Q. Ge, Dynamic redox cycle of Cu0 and Cu+ over Cu/SiO^2 catalyst in ester hydrogenation, RSC Adv. 5 (2015) 37581–37584, https://doi.org/10.1039/c5ra04389a.

[41] Y. Sun, F. Meng, Q. Ge, J. Sun, Importance of the initial oxidation state of copper for the catalytic hydrogenation of dimethyl oxalate to ethylene glycol, ChemistryOpen 7 (2018) 969–976, https://doi.org/10.1002/open.201800225.

[42] G. Cui, X. Meng, X. Zhang, W. Wang, S. Xu, Y. Ye, K. Tang, W. Wang, J. Zhu, M. Wei, D.G. Evans, X. Duan, Low-temperature hydrogenation of dimethyl oxalate to ethylene glycol via ternary synergistic catalysis of Cu and acid–base sites, Appl. Catal. B Environ. 248 (2019) 394–404, https://doi.org/10.1016/j.apcatb.2019.02.042.

[43] Y. Song, J. Zhang, J. Lv, Y. Zhao, X. Ma, Hydrogenation of dimethyl oxalate over copper-based catalysts: acid–base properties and reaction paths, Ind. Eng. Chem. Res. 54 (2015) 9699–9707, https://doi.org/10.1021/acs.iecr.5b01928.

[44] Y. Zhao, Y. Zhang, Y. Wang, J. Zhang, Y. Xu, S. Wang, X. Ma, Structure evolution of mesoporous silica supported copper catalyst for dimethyl oxalate hydrogenation, Appl. Catal. A Gen. 539 (2017) 59–69, https://doi.org/10.1016/j.apcata.2017.04.001.

[45] a) R.-P. Ye, L. Lin, L.-C. Wang, D. Ding, Z. Zhou, P. Pan, Z. Xu, J. Liu, H. Adidharma, M. Radosz, M. Fan, Y.-G. Yao, Perspectives on the active sites and catalyst design for the hydrogenation of dimethyl oxalate, ACS Catal. 10 (2020) 4465–4490, https://doi.org/10.1021/acscatal.9b05477;
b) Y. Wang, W. Yang, D. Yao, S. Wang, Y. Xu, Y. Zhao, X. Ma, Effect of surface hydroxyl group of ultra-small silica on the chemical states of copper catalyst for dimethyl oxalate hydrogenation, Catal. Today 350 (2020) 127–135, https://doi.org/10.1016/j.cattod.2019.06.031.

[46] L.F. Chen, P.J. Guo, M.H. Qiao, S.R. Yan, H.X. Li, W. Shen, H.L. Xu, K.N. Fan, Cu/SiO_2 catalysts prepared by the ammonia-evaporation method: texture, structure, and catalytic performance in hydrogenation of dimethyl oxalate to ethylene glycol, J. Catal. 257 (2008) 172–180, https://doi.org/10.1016/j.jcat.2008.04.021.

[47] J.W. Evans, M.S. Wainwright, A.J. Bridgewater, D.J. Young, On the determination of copper surface area by reaction with nitrous oxide, Appl. Catal. 7 (1983) 75–83, https://doi.org/10.1016/0166-9834(83)80239-5.

[48] M. Thommes, K. Kaneko, A.V. Neimark, J.P. Olivier, F. Rodriguez-Reinoso, J. Rouquerol, K.S.W. Sing, Physisorption of gases, with special reference to the evaluation of surface area and pore size distribution (IUPAC Technical Report), Pure Appl. Chem. 0 (2015), https://doi.org/10.1515/pac-2014-1117.

[49] C.J.G. Van Der Grift, P.A. Elberse, A. Mulder, J.W. Geus, Preparation of silica-supported copper catalysts by means of deposition-precipitation, Appl. Catal. 59 (1990) 275–289, https://doi.org/10.1016/S0166-9834(00)82204-6.

[50] X. Ma, H. Chi, H. Yue, Y. Zhao, Y. Xu, J. Lv, S. Wang, J. Gong, Hydrogenation of dimethyl oxalate to ethylene glycol over mesoporous Cu-MCM-41 catalysts, AIChE J. 59 (2013) 2530–2539, https://doi.org/10.1002/aic.13998.

[51] C.J.G. van der Grift, J.W. Geus, M.J. Kappers, J.H. van der Maas, Characterization of copper-silica catalysts by means ofin Situ diffuse reflectance infrared Fourier transform spectroscopy, Catal. Lett. 3 (1989) 159–168, https://doi.org/10.1007/BF00763725.

[52] J.L.G. Fierro, Chapter 1 Chemisorption of Probe Molecules, in: Studies in Surface Science and Catalysis, 1990, pp. B1–B66, https://doi.org/10.1016/S0167-2991(08)61512-8.

[53] S. Abate, K. Barbera, G. Centi, G. Giorgianni, S. Perathoner, Role of size and pretreatment of Pd particles on their behaviour in the direct synthesis of H_2O_2, J. Energy Chem. 25 (2016) 297–305, https://doi.org/10.1016/j.jechem.2016.01.008.

[54] H. Knozinger, E. Taglauer, Spreading and wetting, in: Handbook of Heterogeneous Catalysis, Wiley-VCH Verlag GmbH & Co. KGaA, Weinheim, Germany, 2008, pp. 29–37, https://doi.org/10.1002/9783527610044.hetcat0027.

[55] S. Li, Y. Wang, J. Zhang, S. Wang, Y. Xu, Y. Zhao, X. Ma, Kinetics study of hydrogenation of dimethyl oxalate over Cu/SiO2 catalyst, Ind. Eng. Chem. Res. 54 (2015) 1243–1250, https://doi.org/10.1021/ie5043038.

[56] C. Xu, G. Chen, Y. Zhao, P. Liu, X. Duan, L. Gu, G. Fu, Y. Yuan, N. Zheng, Interfacing with silica boosts the catalysis of copper, Nat. Commun. 9 (2018), 3367, https://doi.org/10.1038/s41467-018-05757-6.